Bulgarian Chemical Communications, Volume 48, Special Issue E (pp. 77 - 87) 2016

Performance study of a parabolic trough solar collector with an inner radiation shield

Qiliang Wang[1], Gang Pei[*,1], Yang Honglun[1], Anjum Munir[2], Hu Mingke[1]

[1] *Department of Thermal Science and Energy Engineering, University of Science and Technology of China, Hefei 230027, China*

[2] *Department of Energy Systems Engineering, University of Agriculture, Faisalabad-Pakistan*

Parabolic trough collectors (PTCs) have become the most popular technology to harvest solar energy in high-temperature solar thermal utilization areas. The evacuated tube used as the receiver of PTC is the key part and has the highest temperature in the entire system. Heat loss occurs in the evacuated tube at high temperature mainly through thermal radiation, when heat convection and heat conduction are ignored under vacuum condition. This study is a preliminary investigation of a new idea to decrease heat loss by introducing an inner radiation shield at the upper annular vacuum gap, which does not receive concentrated radiation from the parabolic mirrors but receives sunlight directly from the sun. The study presents numerical performance evaluation and comparative analyses based on numerical simulation with and without radiation shields under different environmental conditions, involving the factors of ambient temperature, wind speed, solar irradiance, and so on. The numerical simulation relies on the spectrum parameter model of radiation heat transfer, which has been rarely applied in previous PTC analyses. Results show that, when the working temperature is higher than the critical temperature, the evacuated tube with a radiation shield leads to less radiation heat loss than that without a shield. The converse result is obtained when the working temperature is lower than the critical temperature. The critical temperature is 285 °C in this study when the ambient temperature, wind speed, and solar irradiance are 15 °C, 2.5 m/s, and 800 W/m^2, respectively. When the working temperatures of the tube are 300, 400, 500, and 600 °C, the heat losses from the evacuated collector with a shield are 6.1%, 18.0%, 23.4%, and 25.8% less than the heat losses from that without a shield, respectively.

Keywords: solar energy, parabolic trough collector, radiation shield, heat loss

INTRODUCTION

Parabolic trough collectors (PTCs) represent an advanced technology to harvest solar energy to generate high heat flux, and are applied popularly to areas of solar thermal utilization with high temperature, such as solar thermal power generation system, solar cooling, and solar desalination [1–4].

The evacuated receiver as the key part of PTC is mainly composed of a metal absorber tube with a solar selective absorbing coating on its outer surface, a glass envelope, glass-metal sealing, and a metal bellow [5–6]. To reduce the heat loss by conduction and convection, the annular gap between the metal absorber and the glass envelope is pumped up to vacuum state. In particular, the heat loss that the energy transfers from the receiver to the environment is the sum of heat transfer from the glass envelope, metal bellow, and absorber tube to environment. Moreover, the heat loss of the evacuated receiver is one of the most important parameters to indicate the performance of the receiver, and is a large part of the total heat loss of PTC [5, 7–8]. In reality, the operating temperature can be as high as 400 °C in the system of solar thermal power generation [9]; accordingly, the selective sunlight-absorbing surface coating on the outer surface of the absorber tube is diminished with the increase of temperature because of its higher average emittance in the entire band [10]. This phenomenon leads to excessive radiation losses including that from the absorber tube to the glass envelope and that from the absorber tube through the glass envelope directly to the sky. Specifically, the heat loss of the evacuated receiver deteriorates considerably, thereby resulting in low system operating efficiency. Thus, investigating the heat loss of evacuated receivers is important.

Researchers in relevant fields have attempted to reduce the heat loss of evacuated receivers by improving the performance of selective coating on the absorber tube that possesses low emittance and evacuating the annular of the receiver [11–13]. Another easy and effective way proposed by researchers is introducing a radiation shield to a certain position of vacuum annular, wherein the radiant heat loss intercepted by the radiation shield is larger than the solar irradiation intercepted by the radiation shield. Hany Al-Ansary et al. [14–15] introduced a new PTC with gas-filled annuli. The main idea is to fill the outward-facing half of the gas-filled annulus with a heat-resistant insulating material (fiberglass). They simulated the conduction and convection heat losses from a new PTC receiver and compared them with a conventional receiver with an air-filled annulus. The comparison showed that the heat loss from a

* To whom all correspondence should be sent:
peigang@ustc.edu.cn

receiver using this technique was reduced by a maximum of approximately 25%. Zhang et al. [16] investigated direct-flow coaxial evacuated-tube solar collectors with and without heat shields by experimental performance evaluation and comparative analyses. The test showed that the evacuated tube collector with heat shield had higher optical efficiency, lower heat loss, and better thermal performance compared with that without heat shield.

The PTC receiver intercepts and absorbs the majority of concentrated sunlight at its lower portion, as well as sunlight directly from the sun with low energy density at its upper portion. This fact can be considered to design a new evacuated receiver by introducing a radiation shield to the upper portion of the receiver.

The study investigates the heat loss of two kinds of new evacuated receivers with radiation shields. The study creates a spectrum parameter model of radiation heat transfer, associating the spectral emittance of selective sunlight-absorbing coating and spectral transmittance of the glass envelope. The heat loss by radiation from the absorber tube through the glass envelope to the sky, which is rarely mentioned in previous studies, is also simulated. The simulation is conducted by employing the measurement of the radiation resistance network. The study also presents the numerical evaluation of the heat loss of evacuated tubes with and without radiation shields under different environment conditions and conducted a comparison analysis on both.

SIMULATION MODELS

As stated previously, a radiation shield is introduced to a receiver at the upper outward-facing portion of the vacuum annular space. In this space, the absorber only absorbs the direct solar irradiance. The angle at which the radiation shield surrounds the absorber is set as 120°, the reason for this angle is that the sunlight reflected from the parabolic mirror is ensured to be not intercepted by the radiation shield, as shown in Fig.1. The evacuated receiver without a radiation shield and the two kinds of evacuated receivers with radiation shields are named original evacuated receiver, evacuated receiver I, and evacuated receiver II, for ease of investigation. Evacuated receivers I and II differ in terms of the outer surface material of their radiation shields, selective sunlight-absorbing coating, and polished metal surface. Their inner surfaces are polished metal.

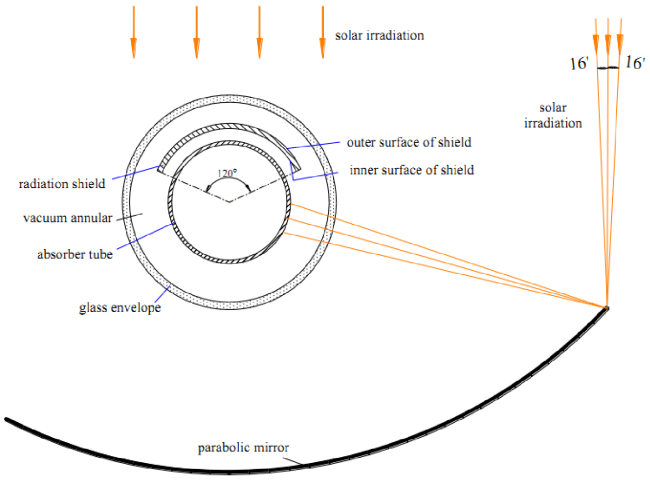

Fig.1. Shcematic cross-section diagram of the PTC system with a new evacuated receiver

The following assumptions are made to simplify the model: ① The heat loss of two ends of the receiver and metal bellow is disregarded, that is, the radiation heat transfer of the evacuated receiver is a 1D heat transfer model. ② The temperature gradient of the glass envelope is ignored because of its thinness. ③ All the involved surfaces in this study are diffusing surfaces. ④ The little natural convection and air conduction in the vacuum annular gap can be satisfied when high vacuum is guaranteed. ⑤ The parabolic trough mirror and concentrated sunlight from the mirror need not reflect in the model because no mutual influence exists between them and the radiation shields. Another reason is that the model is performed under simulated condition in the laboratory. The simplified 1D heat transfer models of the original and new-type receivers are shown in Fig.2.

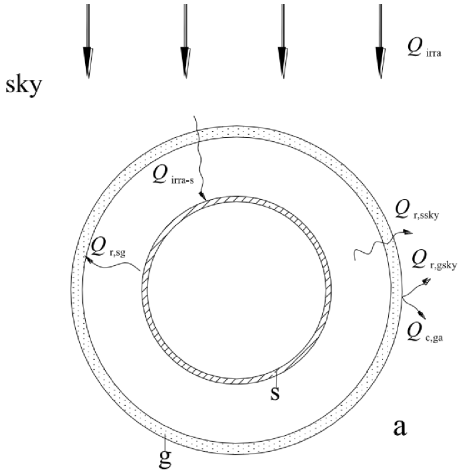

(a)

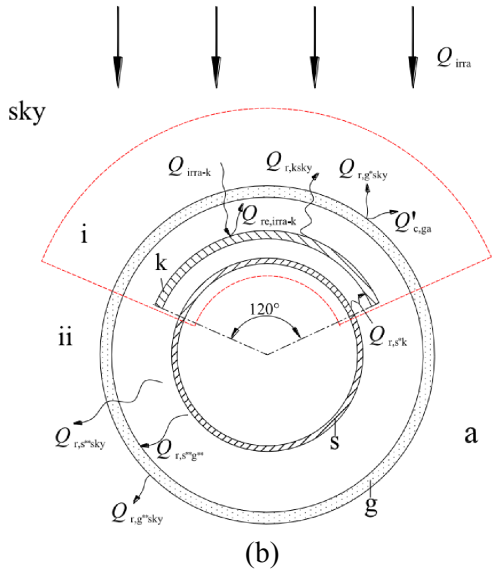

Fig.2. 1D heat transfer model. (a) heat transfer radial cross-section of original receiver, and (b) heat transfer radial cross-section of new-type receiver

Radiation heat transfer model and total heat loss computation model

Simulating the total heat losses of the original and new-type evacuated receivers numerically is the key component to compare and analyze the performance between the two. Radiation heat transfer between the absorber and the sky should also be considered. A large amount of radiation heat losses from the absorber are obtained through the glass envelope directly to the sky, when the PTC receiver operates with a high temperature. This phenomenon occurs because of the increase of radiation power in the solar spectrum wavelength band on the absorber surface. A radiation heat transfer model that employs spectral parameters is established to accurately calculate total heat loss and radiation heat loss between the absorber and the sky. The model is based on a formula derivation of radiation heat transfer by Holman J P [17]. Fig.3 shows the radiation resistance network of the original receiver. The thermal resistances of this receiver are presented in Table 1.

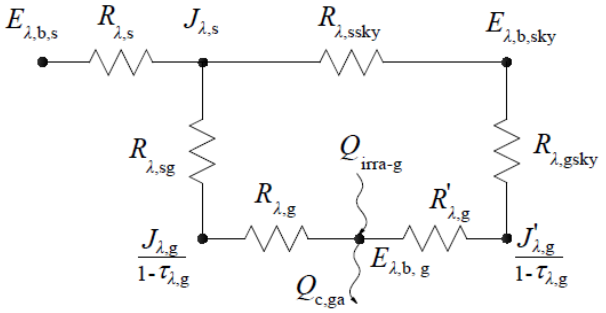

Fig.3. Radiation resistance network of original evacuated receiver

Table 1. Values of equivalent resistances of original evacuated receiver

$R_{\lambda,s}$	$(1-\varepsilon_{\lambda,s})/(\varepsilon_{\lambda,s}A_s)$
$R_{\lambda,sg}$	$1/[A_sF_{sg}(1-\tau_{\lambda,g})]$
$R_{\lambda,gsky}$	$1/[A_gF_{gsky}(1-\tau_{\lambda,g})]$
$R_{\lambda,ssky}$	$1/(A_sF_{ssky}\tau_{\lambda,g})$
$R_{\lambda,g}$	$\rho_{\lambda,g}/[\varepsilon_{\lambda,g}A_g(1-\tau_{\lambda,g})]$
$R'_{\lambda,g}$	$\rho_{\lambda,g}/[\varepsilon_{\lambda,g}A_g(1-\tau_{\lambda,g})]$

To effectively describe and interpret the model mechanism with and without radiation shield, the new-type evacuated receiver is divided into two parts, as shown in Fig.2b. The part surrounded by a red dotted line is called i-zone, and the other part is called ii-zone. The radiation shield in the i-zone of the new-type evacuated receiver corresponds to a new thermal resistance added to the radiation heat resistance network of the original evacuated receiver, as shown in Fig.4. Table 2 presents the corresponding thermal resistances of the new-type evacuated receiver.

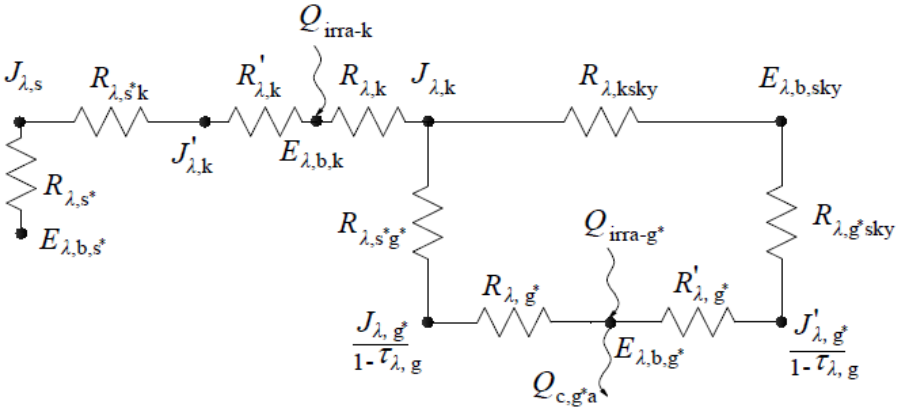

Fig.4. Radiation resistance network in i-zone of new-type evacuated receiver

Table 2. Values of equivalent resistances in i-zone of new-type evacuated receiver

R_{λ,s^*}	$(1-\varepsilon_{\lambda,s})/(\varepsilon_{\lambda,s}A_{s^*})$
R_{λ,s^*k}	$1/(A_{s^*}F_{s^*k})$
$R_{\lambda,k}$	$(1-\varepsilon_{\lambda,ko})/(\varepsilon_{\lambda,ko}A_k)$
$R'_{\lambda,k}$	$(1-\varepsilon_{\lambda,ki})/(\varepsilon_{\lambda,ki}A_k)$
R_{λ,kg^*}	$1/[A_kF_{kg^*}(1-\tau_{\lambda,g})]$
R_{λ,g^*sky}	$1/[A_gF_{g^*sky}(1-\tau_{\lambda,g})]$
$R_{\lambda,ksky}$	$1/(A_kF_{ksky}\tau_{\lambda,g})$
R_{λ,g^*}	$\rho_g/[\varepsilon_{\lambda,g}A_{g^*}(1-\tau_{\lambda,g})]$
R'_{λ,g^*}	$\rho_{\lambda,g}/[\varepsilon_{\lambda,g}A_{g^*}(1-\tau_{\lambda,g})]$

All property parameters of materials including $\varepsilon_{\lambda,g}$, $\tau_{\lambda,g}$, $\rho_{\lambda,g}$, $\varepsilon_{\lambda,ki}$, $\varepsilon_{\lambda,ko}$, and $\varepsilon_{\lambda,s}$, are the functions of wavelength λ, as well as the equivalent thermal resistances and emissive power of blackbody related to the parameters. The values of all property parameters, continuously assigned from 0.36 μm to 100.20 μm per fraction of 0.1 μm, are substituted in networks shown in Fig.2 and Fig.3. The relevant temperatures, including T_a, T_{sky}, T_s, T_g, and T_k, are also essential in solving the models. The emissive power of the blackbody at each node can be obtained from the results of the models. Accordingly, radiation heat flux per unit wavelength at each line of network can be achieved. Table 3 lists the radiation heat flux of each part of the system, that is, the accumulation of radiation heat flux from 0.36 μm to 100.20 μm per fraction of 0.1 μm.

Similarly, the radiation heat transfers in the ii-zone of new-type evacuated receiver, including that between the absorber and the sky, that between the absorber and the glass envelope, and that between the glass envelope and the sky, can be determined by computing the aforementioned heat loss model of the original receiver. Then, the three radiation heat fluxes by integrating both radiation heat fluxes of the i-zone and ii-zone of the new-type evacuated tube can be expressed as

$$Q'_{r,gsky} = Q_{r,g^*sky} + Q_{r,g^{**}sky} \quad (1)$$

$$Q'_{r,(sk)g} = Q_{r,s^{**}g^{**}} + Q_{r,kg^*} \quad (2)$$

$$Q'_{r,(sk)sky} = Q_{r,s^{**}sky} + Q_{r,ksky} \quad (3)$$

The total heat losses of the original and new-type evacuated receivers are as follows:

$$Q_{loss} = Q_{r,gsky} + Q_{c,ga} + Q_{r,ssky} \quad (4)$$

$$Q'_{loss} = Q'_{r,gsky} + Q'_{c,ga} + Q'_{r,(sk)sky} + Q_{re,irra-k} \quad (5)$$

Table 3. Radiation heat fluxes of all parts of system

Types of evacuated receiver	Radiation heat flux
Original evacuated receiver	$Q_{r,ssky} = \sum_{\lambda=0.36}^{100.20} \frac{J_{\lambda,s} - E_{\lambda,b,sky}}{R_{\lambda,ssky}} \times 0.1$
	$Q_{r,sg} = \sum_{\lambda=0.36}^{100.20} \frac{J_{\lambda,s} - E_{\lambda,b,g}}{R_{\lambda,sg} + R_{\lambda,g}} \times 0.1$
	$Q_{r,gsky} = \sum_{\lambda=0.36}^{100.20} \frac{E_{\lambda,b,g} - E_{\lambda,b,sky}}{R_{\lambda,gsky} + R'_{\lambda,g}} \times 0.1$
	$Q_{irra-s} = A_s\alpha_{\lambda,s}\tau_{\lambda,g} \times Q_{irra}$
i-zone of new-type evacuated receiver	$Q_{r,ksky} = \sum_{\lambda=0.36}^{100.20} \frac{J_{\lambda,k} - E_{\lambda,b,sky}}{R_{\lambda,ksky}} \times 0.1$
	$Q_{r,kg^*} = \sum_{\lambda=0.36}^{100.20} \frac{J_{\lambda,k} - E_{\lambda,b,g^*}}{R_{\lambda,kg^*} + R_{\lambda,g^*}} \times 0.1$
	$Q_{r,g^*sky} = \sum_{\lambda=0.36}^{100.20} \frac{E_{\lambda,b,g^*} - E_{\lambda,b,sky}}{R_{\lambda,g^*sky} + R'_{\lambda,g}} \times 0.1$
	$Q_{r,s^*k} = \sum_{\lambda=0.36}^{100.20} \frac{J_{\lambda,s^*} - E_{\lambda,b,sky}}{R_{\lambda,s^*k} + R'_{\lambda,k}} \times 0.1$
	$Q_{irra-k} = A_k\varepsilon_{\lambda,ko}\tau_{\lambda,g} \times Q_{irra}$
	$Q_{re,irra-k} = A_k(1-\varepsilon_{\lambda,ko})\tau_{\lambda,g} \times Q_{irra}$

Iterative computation is applied to calculate the heat loss model based on the thermal equilibrium state of the evacuated receiver. For the new-type receiver, two quantitative expressions are used to model calculation with the given variables T_s, T_g, and T_k. The two expressions incorporate the thermal equilibrium equations of the glass envelope and the radiation shield, as shown in (6) and (7). However, for the original receiver, using one quantitative expression, that is, thermal equilibrium of glass envelope, is enough. This expression is related to the given variables T_s and T_g, and is presented as (8).

$$Q_{r,ksky} + Q_{r,kg^*} = Q_{r,s^*k} + Q_{irra-k} \quad (6)$$

$$Q'_{r,gsky} + Q'_{c,ga} = Q'_{r,(sk)g} + Q_{re,irra-k-g^*} + Q_{irra-g} \quad (7)$$

$$Q_{r,gsky} + Q_{c,ga} = Q_{r,sg} + Q_{irra-g} \quad (8)$$

where $Q_{re,irra-k-g^*}$ refers to solar energy reflected from the radiation shield absorbed by the glass

envelope, that is, it is the product of absorptivity of the glass envelope and $Q_{\text{re,irra-k}}$.

Spectral emissive power

The spectral emissive power of each part of the system, which plays an important linkage role in the calculation of models, is solved by the algorithm of blackbody spectral emissive power [18], as shown in Equation (9).

$$E_{\lambda,\text{b}}(\lambda,T)=\pi I_{\lambda,\text{b}}(\lambda,T)=\frac{C_1}{\lambda^5\{\exp[C_2/(\lambda T)]-1\}} \quad (9)$$

where T is the absolute temperature of the blackbody (K). The first and second radiation constants are C_1=3.742 × 10^8 W·μm^4/m^2 and C_2=1.439 × 10^4 μm·K. $I_{\lambda,\text{b}}(\lambda,T)$ is the blackbody spectral intensity and is expressed as

$$I_{\lambda,\text{b}}(\lambda,T)=\frac{2hc_0^2}{\lambda^5\{\exp[hc_0/(\lambda kT)]-1\}} \quad (10)$$

where h=6.626 × 10^{-34} J·s and k=1.381 × 10^{-34} J/K are the universal Planck and Boltzmann constants, respectively; c_o =2.998 × 10^8 m/s is the speed of light in a vacuum.

Then, the different spectral emissive powers restricted to a certain wavelength, including $E_{\lambda,\text{b,s}}$, $E_{\lambda,\text{b,g}}$, $E_{\lambda,\text{b,k}}$, and $E_{\lambda,\text{b,sky}}$, can be obtained with several related temperatures.

Convection heat transfer

Apart from radiation heat transfer between the glass envelope and ambient, convection heat transfer between the outer surface of the glass envelope and ambient is also an important mode of heat loss in the glass envelope, and is expressed as follows:

$$Q_{\text{c,ga}}=h_c(T_\text{g}-T_\text{a})A_\text{g} \quad (11)$$

For an isothermal cylinder, $h_{\text{c,}}$ the convection heat transfer coefficient of air around the horizontal glass envelope is expressed in the following form:

$$h_c=\frac{K}{D_\text{g}}Nu_D \quad (12)$$

When wind velocity is less than 0.1 m/s, wind flow around the PTC receiver can be regarded as natural convection. Nusselt number N_{uD} can be expressed as

$$Nu_D=\{0.60+\frac{0.387Ra_\text{D}^{1/6}}{[1+(0.559/Pr)^{9/16}]^{8/27}}\}^2 \quad (13)$$

By contrast, wind flow around the PTC receiver can be regarded as forced convection when wind velocity is higher than or equal to 0.1 m/s. The corresponding expression of Nusselt number is

$$Nu_\text{D}=CRe_\text{D}^m Pr^n(\frac{Pr}{Pr_\text{s}})^{1/4} \quad (14)$$

where values of C and m are listed in Table 4. If $Pr\leq 10$, then n=0.37; if $Pr>10$, then n=0.36.

Table 4. Values of C and m with changes of Re_D

Re_D	C	m
0.4–40	0.75	0.4
40–1000	0.51	0.5
1000–2×10^5	0.26	0.6
2×10^5–10^8	0.076	0.7

INVESTIGATION ON Φ102 EVACUATED RECEIVERS AND RESULT ANALYSIS

The Φ102 evacuated receiver provided by Beijing Jindu Solar Energy Tech. Co. Ltd. is used in this study.

Basic parameters of φ102 evacuated receiver

Table 5. Materials of Φ102 evacuated receiver

Name	Material	Dimension
Outer tube	High borosilicate glass	External diameter: 102 mm Internal diameter: 97 mm
Absorber	SUS304 stainless steel	External diameter: 51 mm Internal diameter: 48 mm
Radiation shield	Aluminum sheet	Diameter: 66 mm Angle: 120°

The length of the Φ102 evacuated receiver is 1.98 m and its basic parameters are presented in Table 5. Fig.5a shows the curve of spectral absorptivity of selective sunlight-absorbing coating on the outer surface of the absorber and radiation shield. Fig.5b shows the curve of spectral transmittance of the glass envelope. The emittance of polished aluminum surface is reported in the literature [18].

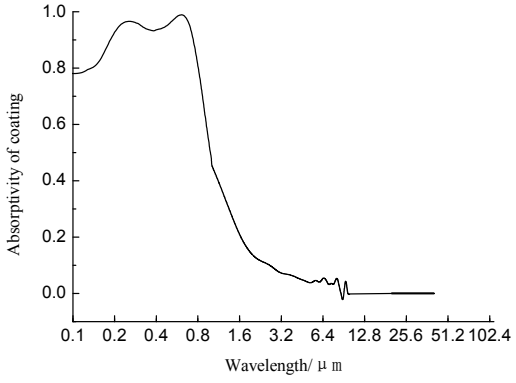

(a)

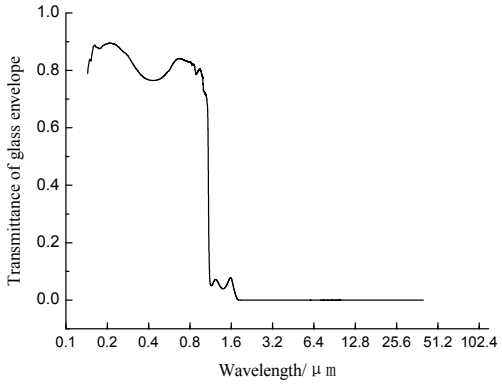

(b)

Fig.5. Spectral properties of physical parameters. (a) spectral absorptivity of selective sunlight-absorbing coating, and (b) spectral transmittance of glass envelope

Analysis of results of heat loss model

The heat loss model in this study is applicable to the test platform under laboratory conditions. The model is based on the investigation of the performance of Schott 2008 PTR70 PTC receiver conducted by NREL [19]. Thus, T_a is equal to T_{sky} under laboratory.

When the ambient temperature, wind speed, and solar irradiance are set as 15 °C, 2.5 m/s, and 800 W/m^2, the heat loss simulations of the original and new-type receivers are conducted at different absorber temperatures varying from 160 °C to 600 °C at 20 °C intervals. The simulation results (40 °C intervals) are presented in Table 6 and Fig.6.

Table 6. Results of heat loss model

T_s/°C	Original receiver		Receiver I				Receiver II			
	Q_{loss} / W·m^{-1}	T_g/°C	Q'_{loss} /W·m^{-1}	T_g /°C	Increments of heat gain / W·m^{-1}	Heat loss reduction /%	Q'_{loss} / W·m^{-1}	T_g /°C	Increments of heat gain /W·m^{-1}	Heat loss reduction /%
160	23.1	17.9	41.7	20.8	–18.6	–80.5	53.3	17.9	–30.2	–130.7
200	39.1	20.0	57.9	23.1	–18.8	–48.1	69.4	18.6	–30.3	–77.5
240	63.8	22.3	75.1	24.9	–11.3	–17.7	85.8	20.7	–22.0	–34.5
280	90.8	25.6	93.0	26.8	–2.2	–2.4	107.2	23.9	–16.4	–18.1
320	136.5	30.5	121.0	30.0	15.5	11.4	135.2	26.8	1.3	1.0
360	195.6	36.8	168.8	34.9	26.8	13.7	180.3	30.8	15.3	7.8
400	271.1	43.4	222.2	40.2	48.9	18.0	232.6	36.1	38.5	14.2
440	374.9	52.5	300.0	46.8	74.9	20.0	305.9	42.6	69.0	18.4
480	512.6	63.9	397.4	54.9	115.2	22.4	410.5	50.8	102.1	19.9
520	681.9	75.5	518.8	63.9	163.1	23.9	522.0	60.1	159.9	23.4
560	899.3	89.7	677.5	74.1	221.8	24.7	676.3	71.9	223.0	24.8
600	1174.0	105.7	871.2	86.5	302.8	25.8	868.3	83.5	305.7	26.0

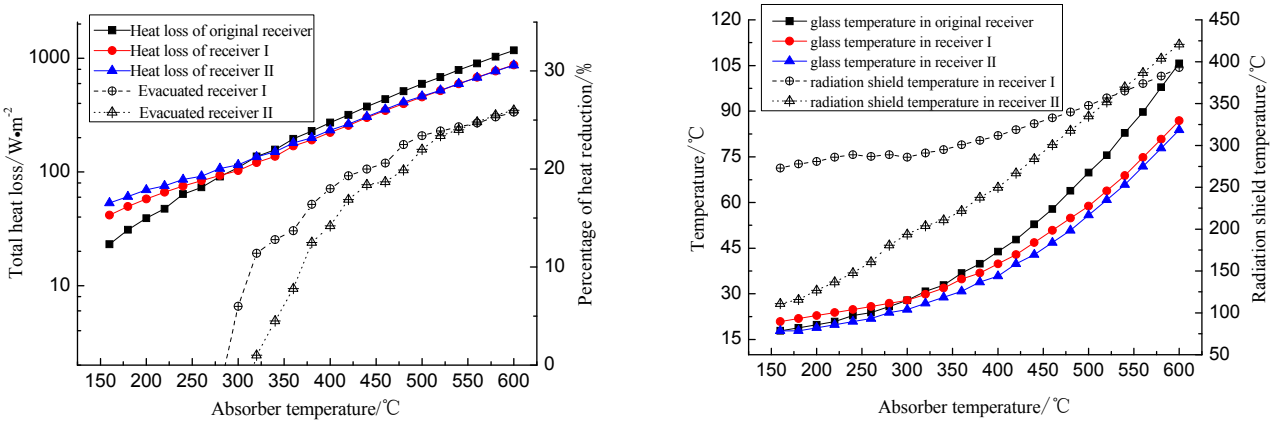

(a) (b)

Fig.6. Simulation results of all kinds of evacuated receivers. (a) values of heat loss varied with absorber temperature, and (b) glass envelope temperature varied with absorber temperature

Table 6 shows that the total heat losses of the original and new-type receivers grow rapidly with the increase of absorber temperature. However, the increments of the two kinds of new-type receivers are larger than that of the original receiver. The four columns of data indicating the heat gain increments and heat reduction percentages of PTC receivers I and II compared with the original PTC receiver increase from negative to positive. This increase shows that the new-type PTC receivers are advantageous to reduce the heat loss of the original PTC receiver at a higher temperature. As the absorber temperature reaches 600 °C, the percentages of heat reduction of the PTC receivers I

and II are 25.8% and 26.0%, respectively. Their increments of heat gain are 302.8 W/m and 305.7 W/m. The increment of heat gain is different between the total heat loss of an original PTC receiver and that of a new-type PTC receiver.

When the absorber is at a lower temperature, the total heat loss of new-type receivers with radiation shield is higher than that of the original receiver. The reason is that radiant energy intercepted and reflected back to the absorber by radiation shield is lower than the incident solar irradiance that should have been absorbed by the absorber if the radiation shield does not exist. However, the increase of absorber temperature gradually increased the intercepted radiant energy, such that the new-type evacuated receiver has less total heat loss than the original receiver. Therefore, the radiation shield starts to come into play. As shown in Fig.6a, the percentage of heat reduction of PTC receiver I is zero when the critical absorber temperature is approximately 285 °C. This finding illustrates that the total heat loss of PTC receiver I is equivalent to that of the original PTC receiver at this critical temperature point. Moreover, the percentage of heat reduction increases dramatically when absorber temperature exceeds 285 °C, given the growing radiant energy intercepted by the radiation shield. Similarly, the critical temperature of the PTC receiver II is approximately 320 °C, which is higher than that of PTC receiver I. Furthermore, the corresponding absorber temperature is nearly 540 °C at the intersection point of the two curves of the total heat loss of PTC receivers I and II. This temperature corresponds to the intersection point of the two curves of heat reduction percentage of receivers I and II. Therefore, two amounts of total heat loss of receivers I and II are equivalent when the absorber temperature is 540 °C. The former is more than the latter because the temperature is lower than 540 °C. However, the converse result is obtained when the temperature is higher than 540 °C.

The aforementioned phenomenon is due to the temperature of the radiation shield in PTC receiver I being higher than that in PTC receiver II at a lower working temperature, as shown in Fig.6b. The reason for this difference is that the coating on the outer surface of the radiation shield in PTC receiver I can absorb most of the incident solar irradiances, but that for the radiation shield of PTC receiver II cannot. In the case of lower working temperature, the transfer direction of the net radiation flux between the absorber and the radiation shield is from the radiation shield with a higher temperature to the absorber. The radiation flux can be regarded as thermal compensation of the intercepted incident solar irradiance for the absorber. In other words, the heat gain of PTC receiver I with higher radiation shield temperature is larger than that of PTC receiver II. This phenomenon explains why the absorber temperature of PTC receiver I compared with PTC receiver II is lower, at which the radiation shield starts to play a role. However, in the case of a higher temperature that exceeds the radiation shield temperature, the role of coating on the surface of the radiation shield decreases. The result from the transfer direction of the net radiation flux is reverse. Thus, the absorber temperature becomes the major factor that affects the temperature of the radiation shield. In addition, the radiative heat loss on the outer surface of the radiation shield in the PTC receiver II appears to increase, but is below that for PTC receiver II. The reason is that the sharply growing coating mean emittance in the entire wavelength is above the increasing mean emittance of polished aluminum outer surface of radiation shield in PTC receiver II. As a result, the shield temperature in PTC receiver II approaches and even exceeds that in PTC receiver I. The absorber temperature is 540 °C, at which the radiation shield temperatures of two kinds of new-type PTC receiver are the same. This phenomenon explains why the difference in the total heat losses of PTC receivers I and II changes before and after 540 °C.

Fig.6b also presents three curves of the relationship between the temperature of glass envelope and absorber temperature. The glass envelope temperature of PTC II is always the lowest by comparing the three curves. The reason lies in the lower radiation heat transfer between the polished outer surface of the radiation shield and the glass envelope.

DISCUSSIONS

All variable parameters used in the models, influencing the performance of PTC receiver, are discussed in this section. These parameters are the transmittance of the glass envelope, ambient temperature, wind velocity, and solar irradiance. Accordingly, we determine whether these parameters have significant influences on the performance of the PTC receiver.

Transmittance of glass envelope

The spectral region in which the radiation is concentrated depends on temperature, with

increased radiation appearing at shorter wavelengths as the temperature rises. Therefore, the value of cumulative emissive power of the absorber at shorter wavelengths is considerable at a higher operating temperature. The majority of value is able to pass through the glass envelope because of high transmittance in the visible region of the solar spectrum maintained by ordinary borosilicate glass. In particular, the $Q_{r,ssky}$ becomes larger with the increase of operating temperature.

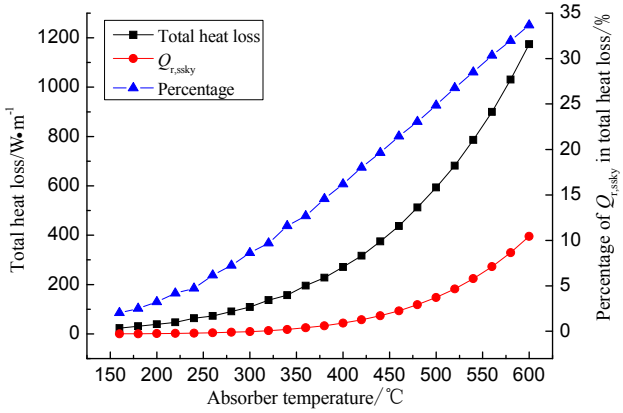

Fig.7. Total heat loss and heat loss transferring through outside glass tube with the changes of absorber temperature

Fig.7 shows the curves of $Q_{r,ssky}$ and total heat loss with varying absorber temperatures, as the ambient temperature, wind speed, and solar irradiance are 15 °C, 2.5 m/s, and 800 W/m^2, respectively. As observed from the curves, the value of $Q_{r,ssky}$ is nearly 0 when the absorber temperature is lower than 400 °C. Then, the value increases significantly as the temperature increases, and the corresponding percentage of $Q_{r,ssky}$ from the total heat loss rises linearly. The percentage reaches 33.7% when the working temperature is 600 °C. Therefore, the radiation heat loss between the absorber and the sky is an important part of total heat loss and cannot be ignored when the operating temperature is higher.

Ambient temperature and wind velocity

In the case where the absorber temperature and solar irradiance are determined, lower ambient temperature and higher wind speed lead to increased heat loss and reduced glass envelope temperature. In fact, the variation of heat loss in an evacuated receiver is insignificantly large with the different ambient temperatures and wind speeds. Heat loss in the glass envelope ($Q_{r,gsky}$+$Q_{c,ga}$) and that between the absorber and the sky ($Q_{r,ssky}$) are two main aspects included in the total heat loss of an original evacuated receiver, according to Formula (4). Moreover, the ($Q_{r,gsky}$+$Q_{c,ga}$) depends on the radiation heat transfer between the absorber and the glass envelope ($Q_{r,sg}$), which is proportional to ($T_s^4 - T_g^4$) as well as $Q_{r,ssky}$ and ($T_s^4 - T_{sky}^4$). $T_s^4 \gg T_g^4$ and $T_s^4 \gg T_{sky}^4$; thus, the decreases of T_g and T_{sky} have a slight influence on the thermal performance of the PTC receiver.

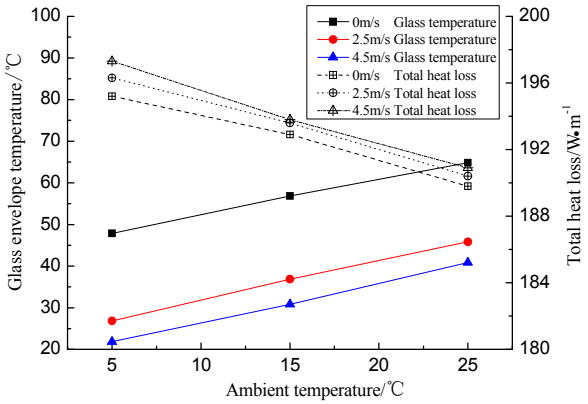

Fig.8. Heat loss of original collector and outside tube temperature with changes of ambient temperature and wind speed (absorber temperature is 360 °C and solar irradiance is 800 W/m^2)

The absorber temperature and solar irradiance are assumed to be 360 °C and 800 W/m^2, respectively; the heat loss and glass temperature are determined for varying laboratory ambient and sky temperatures (5–30 °C) and wind speeds (0–4.5 m/s), as shown in Fig.8. The figure shows that the ambient temperatures and wind speeds can affect the glass temperature by ±25 °C from its average value. However, the heat loss varies slightly with changes in these parameters by ±5 W/m. The difference of respective total heat loss is only 8.5 W/m in the case where ambient temperature is 25 °C and wind speed is 0 m/s, and in the case where ambient temperature is 5 °C and wind speed is 4.5 m/s. Therefore, the heat loss in the PTC receivers is insensitive to the ambient temperature and the wind speed.

Solar irradiance

The radiation shield temperature of PTC receiver I, which affects the heat gain in the absorber associated with the radiant heat loss in the absorber, exhibits a larger variation with the changes in solar irradiance because of the surface coating on it. For PTC receiver I, radiation heat flux $Q_{r,s*k}$ and ($Q_{r,s**g}$+$Q_{r,s**sky}$) are two main parts of heat loss in the absorber according to the simulation model. Smaller net radiation heat flux is obtained in the case where the absorber temperature, ambient temperature, and wind speed are determined. The

reason is that a higher radiation shield temperature is obtained with the increase of solar irradiance. Specifically, the total heat loss in the PTC receiver decreases.

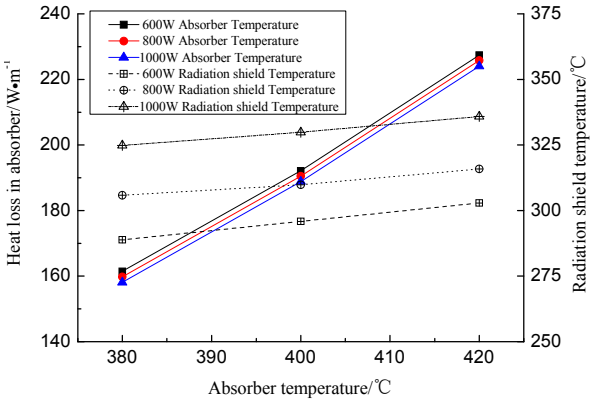

Fig.9. Heat loss in absorber and the radiation shield temperature with varying absorber temperatures (360–420 °C) and solar irradiances (600–1000 W/m^2)

As shown in Fig.9, the heat loss in the absorber and the radiation shield temperature are determined for varying absorber temperatures (360–420 °C) and solar irradiances (600–1000 W/m^2). The figure shows that the solar irradiance can markedly affect the radiation shield temperature by ±15 °C and the heat loss in the absorber by ±2.5 W/m, from their average values at different absorber temperatures. In the case of 400 °C radiation shield temperature, the heat loss in the absorber with solar irradiance 1000 W/m^2 is only 4 W/m, more than that with 600 W/m^2. This phenomenon illustrates that the radiation heat loss in the absorber is insensitive particularly to the radiation shield temperature because of the reduced surface emittances of both the radiation shield inner surface and the absorber outer surface.

CONCLUSIONS

Two kinds of new-type evacuated receivers with inner radiation shield are proposed to improve the performance of the PTC receiver. The study calculates and compares the heat loss of the new-type and original PTC receivers by establishing simulation models based on laboratory conditions. Several important parameters are also analyzed to verify their influence on the performance of the PTC receiver. The obtained conclusions are as follows:

1) The two kinds of new-type PTC receivers can decrease the heat loss in the evacuated receiver. When the working temperature is lower than 540 °C, the receiver with selective sunlight-absorbing coating on the outer surface of the radiation shield is superior to that with polished aluminum outer surface of the radiation shield. However, the latter is superior to the former if the working temperature surpasses 540 °C. In the case where the absorber temperature reaches 600 °C, the heat reduction percentages of both compared with that of the original receiver are 25.8% and 26.0%. Therefore, the two kinds of new-type receiver have remarkable performances.

2) The percentage of radiant heat loss through the glass envelope between the absorber and the sky from the total heat loss increases gradually with the increase of operating temperature. In particular, at a medium-high temperature such as 600 °C, the percentage increases to 33.7%, which should be considered.

3) The lower temperature of the glass envelope is obtained with lower ambient temperature and faster wind speed, but the total heat loss varies slightly if a good vacuum is guaranteed. The difference of respective total heat loss is only 8.5 W/m in the case where ambient temperature is 25 °C and wind speed is 0 m/s, and in the case where ambient temperature is 5 °C and wind speed is 4.5 m/s.

ACKNOWLEDGMENT

This study was sponsored by (1) the National Science Foundation of China (NSFC 51476159 and 51206154), (2) the Dongguan Innovative Research Team Program (No. 2014607101008), and (3) the National Science and Technology Support Program (No. 2015BAD19B02).

The authors are grateful for the support provided by Beijing Jindu Solar Energy Tech. Co. Ltd. and Mr. Ge Hongchuan.

NOMENCLATURE

s Outer surface of inner absorber tube
g Outer (inner) surface of glass envelope
k Radiation shield
s^* Outer surface of inner absorber tube in i-zone
g^* Outer (inner) surface of glass envelope in i-zone
s^{**} Outer surface of inner absorber tube in ii-zone
g^{**} Outer (inner) surface of glass envelope in ii-zone
$\varepsilon_{\lambda,s}$ Spectral emittance on outer surface of inner absorber tube
$\varepsilon_{\lambda,g}$ Spectral emittance on outer (inner) surface of glass envelope
$\alpha_{\lambda,g}$ Spectral absorptivity on outer (inner) surface of glass envelope

$\rho_{\lambda,g}$ Spectral reflectivity on outer (inner) surface of glass envelope

$\tau_{\lambda,g}$ Spectral transmittance of glass envelope

$\varepsilon_{\lambda,ki}$ Spectral emittance on inter surface of radiation shield

$\varepsilon_{\lambda,ko}$ Spectral emittance on outer surface of radiation shield

A_s Area of surface s (m^2)

A_g Area of surface g (m^2)

A_k Area of inner (outer) surface of radiation shield (m^2)

A_{s*} Area of surface s^* (m^2)

A_{g*} Area of surface g^* (m^2)

T_a Ambient temperature (°C)

T_{sky} Sky temperature (°C)

T_s Absorber temperature (°C)

T_g Glass envelope temperature (°C)

T_k Radiation shield temperature (°C)

$R_{\lambda,s}$ Surface radiative resistance of surface s

$R_{\lambda,g}$ Surface radiative resistance of outer surface of glass envelope

$R'_{\lambda,g}$ Surface radiative resistance of inner surface of glass envelope

$R_{\lambda,gsky}$ Space resistance between glass envelope and sky

$R_{\lambda,ssky}$ Space resistance between absorber and sky

$R_{\lambda,sg}$ Space resistance between absorber and glass envelope

R_{λ,s^*} Surface radiative resistance of surface s^* in i-zone of new-type evacuated receiver

$R_{\lambda,k}$ Surface radiative resistance of outer surface of radiation shield in i-zone

$R'_{\lambda,k}$ Surface radiative resistance of inner surface of radiation shield in i-zone

R_{λ,g^*} Surface radiative resistance of outer surface of glass envelope in i-zone

R'_{λ,g^*} Surface radiative resistance of inner surface of glass envelope in i-zone

R_{λ,s^*k} Space resistance between s^* and inner surface of radiation shield in i-zone

$R_{\lambda,ksky}$ Space resistance between outer surface of radiation shield and sky in i-zone

R_{λ,kg^*} Space resistance between outer surface of radiation shield and inner surface of glass envelope in i-zone

R_{λ,g^*sky} Space resistance between outer surface of glass envelope and sky in i-zone

F_{sg} View factor of surface s with respect to inner surface of glass envelope

F_{ssky} View factor of surface s with respect to sky

F_{s*k} View factor of surface s^* with respect to sky

F_{ksky} View factor of outer surface of radiation shield with respect to sky

F_{kg*} View factor of outer surface of radiation shield with respect to inner surface of glass envelope

F_{gsky} View factor of outer surface of glass envelope with respect to sky

$E_{\lambda,b,s}$ Blackbody spectral emissive power of surface s ($W/(m^2 \cdot \mu m)$)

$E_{\lambda,b,g}$ Blackbody spectral emissive power of surface g ($W/(m^2 \cdot \mu m)$)

$E_{\lambda,b,sky}$ Blackbody spectral emissive power of sky ($W/(m^2 \cdot \mu m)$)

E_{λ,b,s^*} Blackbody spectral emissive power of surface s^* ($W/(m^2 \cdot \mu m)$)

$E_{\lambda,b,k}$ Blackbody spectral emissive power of inner (outer) surface of radiation shield ($W/(m^2 \cdot \mu m)$)

E_{λ,b,g^*} Blackbody spectral emissive power of inner (outer) surface of glass envelope ($W/(m^2 \cdot \mu m)$)

$Q_{r,ssky}$ Net radiation heat flux between absorber and sky in original evacuated receiver (W/m)

$Q_{r,sg}$ Net radiation heat flux between absorber and glass envelope in original evacuated receiver (W/m)

$Q_{r,gsky}$ Net radiation heat flux between glass envelope and sky in original evacuated receiver (W/m)

Q_{irra} Solar irradiance (W/m^2)

Q_{irra-s} Solar energy absorbed by absorber tube (W/m)

$Q_{r,ksky}$ Net radiation heat flux between radiation shield and sky (W/m)

$Q_{r,kg*}$ Net radiation heat flux between radiation shield and the part of glass envelope in i-zone (W/m)

$Q_{r,g*sky}$ Net radiation heat flux between the part of glass envelope in i-zone and sky (W/m)

Q_{r,s^*k} Net radiation heat flux between surface s^* and radiation shield in i-zone (W/m)

$Q_{irra\text{-}k}$ Solar energy absorbed by radiation shield (W/m)

$Q_{re,irra\text{-}k}$ Solar energy reflected by radiation shield (W/m)

$Q_{r,s^{**}sky}$ Net radiation heat flux between surface s^{**} and sky (W/m)

$Q_{r,s^{**}g^{**}}$ Net radiation heat flux between surface s^{**} and glass envelope in ii-zone (W/m)

$Q_{r,g^{**}sky}$ Net radiation heat flux between part of glass envelope in ii-zone and sky (W/m)

$Q'_{r,gsky}$ Net radiation heat flux between glass envelope and sky in new-type evacuated receiver (W/m)

$Q'_{r,(sk)g}$ Total net radiation heat flux between surface s^{**}, radiation shield, and glass envelope in new-type evacuated receiver (W/m)

$Q'_{r,(sk)sky}$ Total net radiation heat flux between surface s^{**}, radiation shield, and sky in new-type evacuated receiver (W/m)

$Q_{irra\text{-}g}$ Solar energy absorbed by glass envelope (W/m)

$Q_{re,irra\text{-}k\text{-}g^*}$ Solar energy reflected from radiation shield absorbed by glass envelope (W/m)

Q_{loss} Total heat loss of original evacuated receiver (W/m)

Q'_{loss} Total heat loss of new-type evacuated receiver (W/m)

$Q_{c,ga}$ Convection between glass envelope and environment (W/m)

REFERENCES

1 He Xinnian, Solar thermal application, Hefei: Publishing House of University of Science and Technology of China, 444-466 (2009).

2 Liu Jianmin, Solar energy application, Beijing: Publishing House of Electronics Industry, 303-374 (2010).

3 Behar Omar, Khellaf Abdallah, Mohammedi, Kamal, A review of studies on central receiver solar thermal power plants, Renewable & Sustainable Energy Reviews, Elsevier, 23, (2013).

4 Fernandez-Garcia A., Zarza E., Valenzuela L., Perez M., Parabolic-trough solar collectors and their applications, Renewable & Sustainable Energy Reviews, Elsevier, 14, (2010).

5 Xiong YaXuan, Wu YuTing, Ma ChongFang, et al., Numerical investigation of thermal performance of heat loss of parabolic trough receiver. Science China-Technological Sciences, Elsevier, 53, (2010).

6 Kalogirou, SA., Solar thermal collectors and applications. Progress in Energy and Combustion Science, Elsevier, 30, (2004).

7 Luepfert Eckhard, Riffelmann Klaus-J., Price Henry, et al., Experimental analysis of overall thermal properties of parabolic trough receivers, Journal of Solar Energy Engineering-Transactions of the ASME, Elsevier, 130, (2008).

8 Mills D., Advances in solar thermal electricity technology, Solar Energy, Elsevier, 76, (2004).

9 Nishith B. Desai, Santanu Bandyopadhyay, Optimization of concentrating solar thermal power plant based on parabolic trough collector, Journal of Cleaner Production, Elsevier, 89, (2015).

10 Xie Guangning, et al., A summary on middle-high temperature solar selective absorbing surface, Proc of ICEA2001[C], Wuhan, China, (2001).

11 Caron S., Roeger M., Pernpeintner J., Transient infrared thermography heat loss measurements on parabolic trough receivers under laboratory conditions, International Conference on Concentrating Solar Power and Chemical Energy Systems, Beijing, Peoples R China, (2014).

12 Pigozzo Filho, Victor C., de Sa, Alexandre B., Passos, Julio C., et al., Experimental and numerical analysis of thermal losses of a parabolic trough solar collector, ISES Solar World Congress (SWC), Cancun, MEXICO, (2013).

13 Daniel Premjit, Joshi Yashavant, Das Abhik K., Numerical investigation of parabolic trough receiver performance with outer vacuum shell, Solar Energy., Elsevier, 85, (2013).

14 Hany Al-Ansary, Obida Zeitoun, Heat Loss Experiments on a Non-Evacuated Parabolic Trough Receiver Employing a Thermally Insulating Layer in the Annular Gap, ASME 2013 7th International Conference on Energy Sustainability collocated with the ASME 2013 Heat Transfer Summer Conference and the ASME 2013 11th International Conference on Fuel Cell Science, Engineering and Technology, Minneapolis, Minnesota, USA, (2013).

15 Hany Al-Ansary, Obida Zeitoun, Numerical study of conduction and convection heat losses from a half-insulated air-filled annulus of the receiver of a parabolic trough collector. Solar energy, Elsevier, 85, (2011).

16 Xin Zhang, Shijun You, Hongchuan Ge, et al., Thermal performance of direct-flow coaxial evacuated-tube solar collectors with and without a heat shield, Energy Conversion and Management, Elsevier, 84, (2014).

17 Holman J P. Heat transfer, New York: McGraw-Hill Inc, 420-460, (1997).

18 Incropera F P, DeWitt D P, Fundamentals of heat and mass transfer, 6th edition, New York: John Wiley and Sons, (1990).

19 Burkholder F, Kutscher C, Heat loss testing of Sehott's 2008 PrR70 parabolic trough receiver [EB／OL], http://www.rtrel.gov/esp/troughnet/pdfs/45633.pdf,2009-05/2009-07.